JOURNAL OF MATERIALS SCIENCE 20 (1985) 1842–1846

# The formation of the high-melting TiN–Ti composites in the pulse plasma

A. MICHALSKI, A. SOKOŁOWSKA
*Institute of Materials Science and Engineering, Warsaw Technical University,*
*ul. Narbutta 85, 02-524 Warsaw, Poland*

The composite layers of titanium and its high-melting compounds ($TiN_x$, $TiN_xC_y$) were crystallized from the pulse plasma on steel at a temperature $\leqslant 500$ K. It was found that the electrode tip was a source of the composite metallic part and that the electrode lateral surfaces covered by titanium compounds yielded vapours of the elements being components of the compound. These vapours were the source of the second composite part. Considering that the type of crystallized layer is determined by temperature and pressure in the nucleation region, one can assume that the TiN nucleation takes place in this very plasma, in the temperature range 1800 to 2700 K.

## 1. Introduction

This paper is a continuation of our studies concerning the crystallization of high-melting compound layers from the pulse plasma [1–3]. The plasma was produced as a result of a pulse discharge of a capacitor battery between two coaxial electrodes in a gas under reduced pressure. This gas and the products of electro-erosion of the central electrode served as substrates for the synthesis of high-melting materials. The greatest advantage of the pulse plasma crystallization method in comparison with many other CVD and PVD methods is the possibility of the deposition of high-melting materials on substrates kept at rather low temperatures ($T \leqslant 500$ K). TiN–Ti layers so deposited on steel (e.g. drills) show excellent antifriction properties. With regard to this application the study of the TiN crystallization mechanism in the pulse plasma is of particular interest. The investigations reported here were made to find the effect of the eroding electrode material and the reactive gas on the phase composition of layers deposited on target placed *vis à vis* the plasma generator outlet as also of materials collected on a substrate placed parallel to the axis at a certain distance from it.

## 2. Experimental details

The layers were obtained with the use of the former described plasma accelerator [1]. Parameters of the deposition process of crystallized products (the energy stored up in the capacitors battery being 10 kJ, and the pressure in the deposition chamber being 20 Pa) were so chosen as to obtain as intense electron-erosion of the central electrode as possible. Crystallization products were deposited on samples of carbon steel (0.45% C) placed opposite the plasma accelerator and distanced 200 mm from it, and on samples placed at the same distance parallel to the axis of plasmoid flight. The substrate temperature during deposition did not exceed 500 K [1, 3]. The materials used for the electrode and reactive gases were tabulated in Table I. Apart from the reactive gas, hydrogen was used with a view to the experimental data stated previously: more efficient electro-erosion of the hot electrode and prevention of the oxide formation, made possible the application of commercially pure gases.

In the conditions described above the compact ultrafine grained layers, ideally adhering to the substrate as described in [1], were obtained. Analysis of the phase composition of the layers showed, in all cases, differentiation of this composition according to the substrate situation. One could always distinguish a region of diameter 50 mm, labelled region A further on, lying symmetrically with respect to the system axis (axis of eroding electrode) on a sample placed perpendicular to the axis and a region called B on a

0022–2461/85 $03.00 + .12

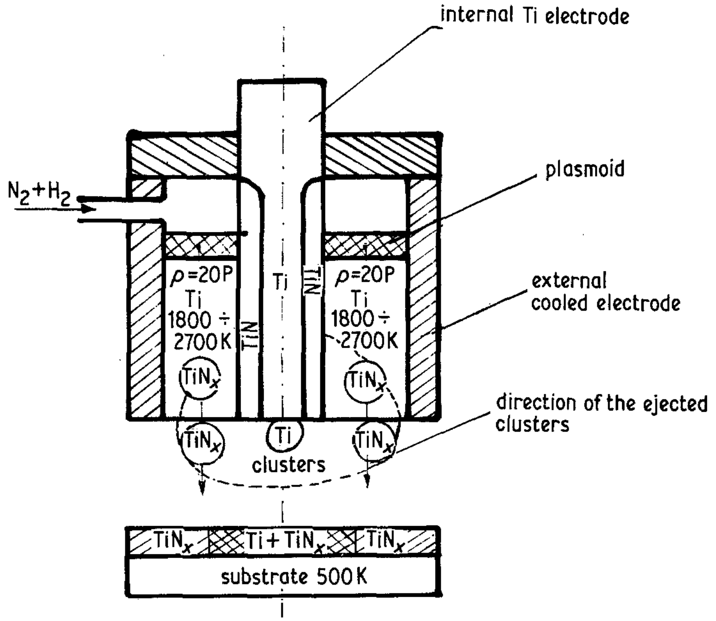

*Figure 1* Arrangement of targets by the deposition process: (1) coaxial plasma accelerator, (2) eroding electrode, (3) region A, (4) region B.

sample placed parallel to the axis and distanced 25 mm from it (Fig. 1).

## 3. Results and discussion

### 3.1. Crystallization in the system Ti–$N_2$

Carrying the crystallization with the use of a titanium electrode in the reactive gas $N_2 + H_2$ we have obtained:

(a) A phase mixture in region A (Fig. 2). One phase is $TiN_x$ with a lattice parameter $a = 0.4266$ nm. This parameter is greater than the maximum value for TiN corresponding to the ratio N/Ti = 1 [4]. The second identified phase was a solid solution of nitrogen in titanium. The ratio of the lattice parameters of this solid solution of nitrogen in titanium $c/a = 1.61$ pointed at ~ 10% of nitrogen dissolved in titanium, after [5].

(b) In region B only a $TiN_{0.55}$ phase with the lattice parameter $a = 0.4227$ nm.

Thus in the system of the hot titanium electrode and the reactive gas $N_2$, a layer composed of the products of a chemical reaction between the electrode vapours and the gas, as well as the solidified vapours of material of nothing but the electrode, was obtained *vis à vis* the electrode end. Layers composed of only $Ti + N_2$ chemical reaction products were obtained in regions at a distance from the electrode axis.

The result indicated that the front face of the hot electrode was the main source of the chemically unchanged titanium, with vapours of the lateral surface layer making a source of titanium chemical compounds.

TABLE I Materials used in experiments

| Electrode material | Reactive gas |
|---|---|
| Commercially pure titanium | $N_2:H_2 = 10:1$ |
| Titanium covered by a layer of titanium carbide | $N_2:H_2 = 10:1$ |
| Titanium covered by a layer of titanium nitride | $CH_4$ |

### 3.2. Crystallization in the system TiC–$N_2$

Carrying the crystallization process with the use of the eroding electrode of titanium covered by a TiC layer and reactive gas mixture $N_2 + H_2$ we have obtained:

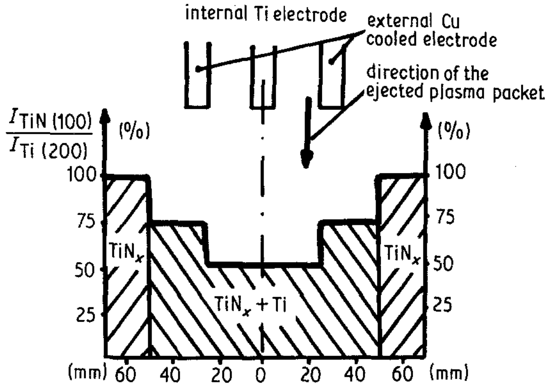

*Figure 2* Radial distribution of the phase content of the layer (region A).

TABLE IIA Diffraction data of layers obtained in the system TiC–$N_2$: A region

| Observed phase | | TiN ASTM card 6-0542 | | Ti ASTM card 5-682 | |
|---|---|---|---|---|---|
| $d$ (nm) | $I/I_0$ | $d$ (nm) | $I/I_0$ | $d$ (nm) | $I/I_0$ |
| 0.254 | 20 | – | – | 0.2557 | 30 |
| 0.243 | 100 | 0.244 | 77 | – | – |
| 0.235 | 100 | – | – | 0.2342 | 26 |
| 0.223 | 60 | – | – | 0.2244 | 100 |
| 0.210 | 60 | 0.212 | 100 | – | – |
| 0.173 | 15 | – | – | 0.1726 | – |
| 0.149 | 15 | 0.1496 | 56 | – | – |
| 0.133 | 15 | – | – | 0.1332 | 16 |
| 0.127 | 15 | 0.1277 | 26 | 0.1276 | 2 |
| 0.122 | 10 | 0.1223 | 16 | 0.1233 | 13 |

(a) In region A a phase mixture composed of $TiN_{0.45}$ with lattice parameter $a = 0.4219$ nm, and titanium (Table II). Investigations of the elements distribution with the use of an electron microprobe along a cross-section of the layer showed a uniform titanium and nitrogen distribution in the whole layer thickness and the existence of a small amount of carbon. One could suppose that this amount was less than 2 at % because the level of carbon signal was lower than that of the substrate containing 2 at % C.

(b) In region B the phase $TiN_{0.8}$ has lattice parameter $a = 0.4234$ nm (Table II).

The result seems to point out that TiN was the most stable of the phases formed under the process conditions from the plasma generated in the titanium, carbon and nitrogen vapours. Comparing the temperature dependences of TiN, TiC and $TiN_xC_y$ formation enthalpy in this atmosphere after the data given in [7] one can state that TiN is the most stable phase up to 1800 K, $TiN_xC_y$ phase can arise in the range 1800 to 2700 K, only TiC is the most stable phase in the system above 2700 K.

The fact that TiC was not obtained in the experiment can be explained by two reasons:

(a) Temperature in the nucleation region did not attain 2700 K;

TABLE IIB Diffraction data of layers obtained in the system TiC–$N_2$ : B region

| Observed phase | | TiN ASTM card 6-0642 | |
|---|---|---|---|
| $d$ (nm) | $I/I_0$ | $d$ (nm) | $I/I_0$ |
| 0.245 | 100 | 0.244 | 77 |
| 0.212 | 90 | 0.212 | 100 |
| 0.150 | 50 | 0.1496 | 56 |
| 0.128 | 20 | 0.1277 | 26 |

TABLE IIIA Diffraction data of layers obtained in the system TiN–$CH_4$: A region

| Observed phase | | TiN ASTM card 6-0642 | | Ti ASTM card 5-682 | |
|---|---|---|---|---|---|
| $d$ (nm) | $I/I_0$ | $d$ (nm) | $I/I_0$ | $d$ (nm) | $I/I_0$ |
| 0.244 | 100 | 0.244 | 77 | – | – |
| 0.225 | 100 | – | – | 0.2244 | 100 |
| 0.212 | 70 | 0.212 | 100 | – | – |
| 0.150 | 30 | 0.1496 | 56 | – | – |
| 0.128 | 25 | 0.1277 | 26 | – | – |
| 0.122 | 10 | 0.1223 | 16 | – | – |

(b) Vapours of the lateral surface of the hot electrode, being the only source of carbon in this experiment, were not efficient enough in supplying the material for crystallization.

The next experiment (Section 3.3) was to afford information as to which of the above mentioned reasons was true.

## 3.3. Crystallization in the system TiN–$CH_4$

Carrying the crystallization with the use of an eroding titanium electrode covered with a titanium nitride layer in the reactive gas $CH_4$ we obtained:

(a) In region A a phase mixture composed of $TiN_{0.8}$ with lattice parameter $a = 0.4235$ nm, and titanium (Table III). Investigations of the elements distribution with the use of the electron microprobe along the layer cross-section showed uniform titanium and nitrogen distribution in the whole layer thickness and a small carbon content ~ 2 at %.

(b) In region B only one complex phase $TiN_xC_y$ (Table III) with the lattice parameter $a = 0.4246$ nm pointing at a TiC content ~ 10 at % [6].

The result of the experiment points at the fact that vapours of the material covering lateral sides of the hot electrode are a competitive source of substrates for the plasma chemical reaction regard-

TABLE IIIB Diffraction data of layers obtained in the system TiN–$CH_4$: B region

| Observed phase | | [6] | |
|---|---|---|---|
| $d$ (nm) | $I/I_0$ | mol % of TiC in TiN | $a$ (nm) |
| 0.248 | 100 | 0 | 0.424 |
| 0.214 | 80 | 20 | 0.426 |
| 0.151 | 75 | 40 | 0.4275 |
| | | 60 | 0.4292 |
| | | 80 | 0.431 |
| | | 100 | 0.433 |

$a = 0.4246$ nm.

TABLE IV Calculated dependence of the TiN critical nucleus radius on temperature (pressure 20 Pa)

| Temperature, $T$ (K) | Vapour pressure above flat surface, $p$ ($10^2$ Pa) | $\ln \frac{p}{p_\infty}$ | Critical nucleus radius, $r_{\text{crit}}$ (nm) |
|---|---|---|---|
| 1800 | $1.33 \times 10^{-3}$ | 5 | 0.7 |
| 2000 | $1.47 \times 10^{-2}$ | 2.6 | 1.26 |
| 2500 | 2.58 | $-2.6$ | – |

ing the gas used in the process. So the phase composition of the layer obtained, as in the test described in Section 3.2, is determined by the temperature of the nucleation region.

On the basis of thermodynamical data one can state that the phases observed are stable at the following temperature ranges: TiN up to 1800 K, and $TiN_xC_y$ from 1800 to 2700 K. Phase TiC, not found in the experiment, is the only phase stable above 2700 K.

## 4. Deduced TiN nucleation conditions

Since in our experiments we have obtained $TiN_x$ or $TiN_xC_y$ we supposed that nucleation took place at a temperature higher than 1800 K and lower than 2700 K. The assumptions that the plasma thermodynamic temperature was the same seems to be reasonable (temperature of the deposition substrate was not higher than 500 K). Assuming homogeneous nucleation of TiN in the plasma, we calculated the radius of critical nucleus $r_{\text{crit}}$ from the Gibbs–Thomson expression

$$r_{\text{crit}} = \frac{2\sigma M}{\rho R T \ln \frac{p}{p_\infty}}$$

where $\sigma$ is the surface tension, $M$ is the molecular weight, $p_\infty$ is the vapour pressure above flat surface, $T$ is temperature, $\rho$ is density, $R$ is the gas constant, and $p$ is the chamber pressure.

We calculated $r_{\text{crit}}$ of TiN nucleus for the temperature range 1800 to 2700 K and pressures 20 Pa assuming $\sigma = 2310 \times 10^{-3}$ J m$^{-2}$ [8], and $p_\infty$ values at various temperatures, after [4]. The results were drawn up in Table IV. Supersaturation calculated for the pressure lower than 20 Pa assumed negative values. The same was true for $p = 20$ Pa and $t \geqslant 2500$ K.

The calculated value of $r_{\text{crit}}$ for TiN agreed quite well with the observed grain dimensions of the thin layers in [3], whose mean radius was $\bar{r} = 7.5$ mm.

## 5. Conclusions

Employing electro-erosion as a source of crystallization substrates we obtained layers which were either composites of titanium and $TiN_x$, or contained only $TiN_x$ contingently on the spatial situation of the substrate regarding the plasma generator. On that basis we can propose the following mechanism of the supply of substrates from the electrode to the crystallization process:

The front face of the internal electrode is a source of its own metal vapours. From these vapours crystallization of titanium only proceeds. This is evidenced by titanium present on surface A and its increasing amount in the substrate centre, exactly opposite the electrode tip. Titanium appears in region A independently on the chemical composition of a surface layer on the electrode.

The lateral surface of the electrode is the source of vapours of the layer covering it. As it has been shown in another paper [9] in the case when the product of the chemical reaction between plasma and the electrode material was a high-melting one, this product deposited on the electrode. Vapours of the surface layers make a source of substrates

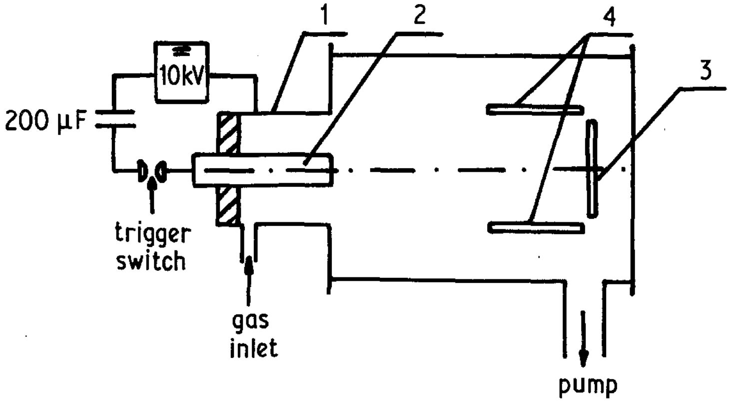

*Figure 3* Schematic presentation of the pulse plasma crystallization process of TiN–Ti composite, proposed on the basis of our investigation.

for plasma crystallization of these compounds onto the substrate. This is manifested by the fact that region B shows the appearance of only $TiN_x$ or $TiN_xC_y$ according to the gas composition and surface layer on the electrode.

The pulse plasma used in experiments was a non-equilibrium one, and its excitation temperature attained $10^4$ K. With a view to the temperature range of thermodynamic stability of the condensed matter, one can suppose that a homogeneous nucleation of TiN takes place in this very plasma. Then the thermodynamic temperature of the plasma where the chemical reaction (cluster formation) takes place ought to range 1800 to 2700 K. The homogeneous nucleation could proceed in that plasma only under pressures higher than 20 Pa.

In the Fig. 3 a schema is shown representing the phenomena taking place during the TiN–Ti crystallization in the pulse plasma.

## Acknowledgement

This work was supported by the Polish Ministry of Science, Higher Education and Technology under contract MRI.21.

## References

1. A. MICHALSKI, *J. Mater. Sci. Lett.* **3** (1984) 505.
2. M. SOKOŁOWSKI, A. SOKOŁOWSKA, A. MICHALSKI, Z. ROMANOWSKI, A. RUSEK-MAZUREK and M. WRONIKOWSKI, *Thin Solid Films* **80** (1981) 249.
3. A. MICHALSKI and Z. ROMANOWSKI, *J. Cryst. Growth* **61** (1983) 675.
4. G. V. SAMSONOV, "Nitridy" (Naukova Dumka, Kiev, 1969) p. 138.
5. S. STOLARZ, "Wysokotopliwe Związki i Fazy" (Śląsk, Katowice, 1974) p. 80.
6. V. N. TROICKIJ, B. M. GREBCOV, J. A. DOMASNEV and S. V. GUROV, in "Plazmochemiceskie Reakcii i Processy", edited by L. S. Polak (Nauka, Moscow, 1977) p. 26.
7. J. V. ZALITE, E. A. PALCEVSKIS and JÁ. P. GRABIS, *Fiz. Chim. Obrabotki Mater.* **1** (1980) 62.
8. P. S. KISLYJ and M. A. KUZENKOVA, "Spekanie Tugoplavkich Sojedinenij (Naukova Dumka, Kiev, 1980) p. 30.
9. M. SOKOŁOWSKI, A. SOKOŁOWSKA, A. RUSEK, A. MICHALSKI and J. GLIJER, *J. Mater. Sci.* **14** (1979) 841.

*Received 16 July*
*and accepted 31 July 1984*